Asian Journal of Chemistry; Vol. 36, No. 6 (2024), 1251-1264

ASIAN JOURNAL OF CHEMISTRY

https://doi.org/10.14233/ajchem.2024.31296

Charge Transfer Complexes of 1-Cyclohexylpiperazine as Donor with 2,3-Dichloro-5,6-dicyano-*p*-benzoquinone and 2,3,5,6-Tetra chloro-*p*-benzoquinone as Acceptors: A Comparative Studies of Spectroscopic, Thermodynamic and DFT Analysis

VENUGOPAL ABBU[1,*], VENKATESH NAMPALLY[2], RAMAKANTH PAGADALA[1,*], SAMBHANI NAGA GAYATRI[1], THIRUPATHI DAMERA[1] and T. PARTHASARATHY[2]

[1]Chemistry Division, Department of Humanities and Science, C.V.R. College of Engineering, Hyderabad-501510, India
[2]Department of Chemistry, Osmania University, Tarnaka, Hyderabad-500007, India

*Corresponding authors: E-mail: abbuvenu@yahoo.com; pagadalaramakanth@gmail.com

Received: 27 January 2024; *Accepted*: 29 March 2024; *Published online*: 31 May 2024; AJC-21635

Novel 1-cyclohexylpiperazine charge transfer compounds, acting as donors, were investigated in conjunction with the π-acceptors 2,3-dichloro-5,6-dicyano-*p*-benzoquinone (DDQ) and 2,3,5,6-tetrachloro-*p*-benzoquinone (CHL) through spectrophotometric analysis at room temperature in acetonitrile. The Benesi-Hildebrand equation was applied to determine the molar extinction coefficient (ε) and stability constant (K_{CT}) for both charge transfer (CT) complexes, each exhibiting a 1:1 molar composition. The infrared (IR) spectroscopy confirmed the presence of CT complexes and these complexes were further evaluated for their pharmacological potential in DNA binding studies, revealing their interaction with DNA through intercalation. The density functional theory (DFT) analysis provided insights into bond lengths, bond angles, Mulliken atomic charges, molecular electrostatic potential (MEP) maps and the highest occupied molecular orbital to the lowest unoccupied molecular orbital (HOMO-LUMO) characteristics of the CT complexes.

Keywords: *p*-Benzoquinones, Charge transfer complexes, Benesi-Hildebrand equation, DFT analysis.

INTRODUCTION

Charge transfer (CT) complexes [1-3] were created using weak interactions between π-electrons acceptor and organic electron donor molecules. These interactions are frequently linked to the production of coloured complexes that absorb visible light [4,5]. The importance of heteroatom donors and acceptors, such as N, O and S atoms in the creation of CT complexes, has increased in recent years [6,7]. The significance of charge transfer complexes has increased in materials research, finding applications in areas such as superconductors and photocatalysis [8], organic semiconductors, related to LEDs [9,10], photovoltaic cells [11], as well as biological significance [12]. Due to their conductivity and optical characteristics, these complexes can be utilized as mechanisms for drug binding [13]. The CT complexes have earned a lot of attention recently in the field of CT-DNA binding [14-16], research on antibacterial and antimicrobial resistance, as well as pharmacological evaluation [17,18].

Piperazines and substituted piperazines are commonly found in physiologically active chemicals as a major component. The electron support possessions of substituted piperazines are enhanced by positive inductive and hyperconjugative effects. Several CT complexation investigations have utilized piperazines and substituted piperazines as donors with different acceptors [19]. For a wide range of applications, 2,3-dichloro-5,6-dicyano-*p*-benzoquinone (DDQ) and 2,3,5,6-tetrachloro-*p*-benzoquinone (CHL) electron acceptors are often used in the chemical synthesis. Benzoquinones have been utilized as electron acceptors with various electron donors to create CT-complexes during the last few decades [20]. These acceptors were thoroughly studied with a variety of donors [21] and resulting in free radical ion pair formation due to transfer of electrons from donor to acceptor. Pharmacological opportunities may result from studies on DNA binding, and most pharmaceutical treatments target them as a key biological target [22]. The binding mechanism of CT-complexes with DNA is critical for both medicinal and scientific applications, as these complexes

interact with DNA through both covalent and non-covalent interactions. Two novel charge transfer complexes were developed in the present study, where donor 1-cyclohexylpiperazine (1-CYHP) was combined with π-acceptors *viz.* 2,3-dichloro-5,6-dicyano-*p*-benzoquinone (DDQ) and 2,3,5,6-tetrachloro-*p*-benzoquinone (CHL).

EXPERIMENTAL

High grade chemicals were used for the experimentation. Sigma-Aldrich, USA provided 1-cyclohexylpiperazine (97%), acceptors, DDQ (98%) and CHL (98%). The calf thymus DNA (Sisco Research Laboratory), tris-buffer (Molechem) and sodium chloride (99.5% SDFCL), while analytical grade methanol (98%, Merck), DMSO (99.9%, Merck) and acetonitrile (99.9%, Merck) solvents were procured. The electronic absorption spectra in the range 250-750 nm were verified using a UV-vis spectrophotometer (Shimadzu UV-2600 model). Using Perkin-Elmer Infrared, the FT-IR spectra was analyzed in the region 4000-500 cm^{-1}.

Synthesis of [(1-CYHP)(DDQ)] and [(1-CYHP)(CHL)]: Charge transfer complex {CTC1: [(1-CYHP)(DDQ)]} was prepared by mixing standard solutions of 1-CYHP and DDQ in a graduated flask and stirred continuously for 1 h. Later the solution was allowed to dry for few days and the obtained gel like solid was used for characterization similarly, solid CTC2: [(1-CYHP)(CHL)] was prepared by mixing standard solutions of 1-CYHP and CHL and the obtained solid was used for characterization. It was observed that solid CTC2 was easily prepared as compared to CTC1.

Preparation of CT-DNA stock solution: Electronic absorption spectra was used to evaluate the DNA binding studies of CT complexes using a UV-vis spectrophotometer. A CT-DNA stock solution was prepared with 5 mM Tris-HCl and 50 mM NaCl in double distilled water. A clear solution was generated after stirring the CT-DNA solution overnight and then filtered and stored. In 10 mM Tris-HCl buffer (pH 7.2), the ratio of CT-DNA absorbance at 260 and 280 nm was 1.8-1.90, implying that the CT-DNA was sufficiently protein-free. Moreover, CT-concentration CT-DNA was calculated using its absorption intensity at 260 nm and a molar extinction value of 6600 M^{-1} cm^{-1}. The titration was performed by increasing the concentration of CT complexes (CTC1 & CTC2) from 0 to 10 μM while keeping CT-DNA (40 μM) constant.

Computational studies: Density functional theory (DFT) studies of the acceptors DDQ, CHL as well as the donor 1-CYHP and CT complexes, CTC1 and CTC-2 were studied in gas phase by using the Gaussian09 w software. The geometry optimization was done with 6-31G and Becke3-Lee-Yang-Parr hybrid exchange correlation three parameter functional (B3LYP) and for generating geometries of molecules, Gauss View 5.0.8 was utilized as an input file.

Mulliken atomic charges of CTC1 and CTC2 were also estimated. In gas phase, optimized geometrical parameters, such as bond angles, bond lengths, molecular electrostatic potential map values and surfaces of occupied and unoccupied molecular orbitals were evaluated.

Usual stock solutions: The regular solutions of donor, 1-cyclohexylpiperazine (0.058 M) was prepared by dissolving 0.25 g (density = 0.969 g/cc) in 25 mL volumetric flask using acetonitrile as solvent. Acceptors, DDQ (1.0×10^{-2} M) and CHL (1.0×10^{-2} M) were prepared by dissolving 0.023 g and 0.025 g, respectively in 10 mL volumetric flask with acetonitrile as solvent. Various standard stock solutions of donor and acceptors were also prepared by diluting with the acetonitrile solvent.

RESULTS AND DISCUSSION

The radical ion pair is formed by the interaction of the donor 1-cyclohexylpiperazine, (1-CYHP) with acceptors DDQ and CHL during the formation of CT-complexes. The movement of electrons from 1-CYHP to the acceptors results in the establishment of brightly coloured CT complexes [23]. The high ionization potential of the donor (1-CYHP) is responsible in the development of CT complexes.

Electronic absorption spectra: The UV-visible electronic absorption spectra of the CT complexes, donor (1-CYHP) and acceptors (DDQ, CHL) are shown in Fig. 1. In both CTCs, the n-π* transition is responsible for the development of two new

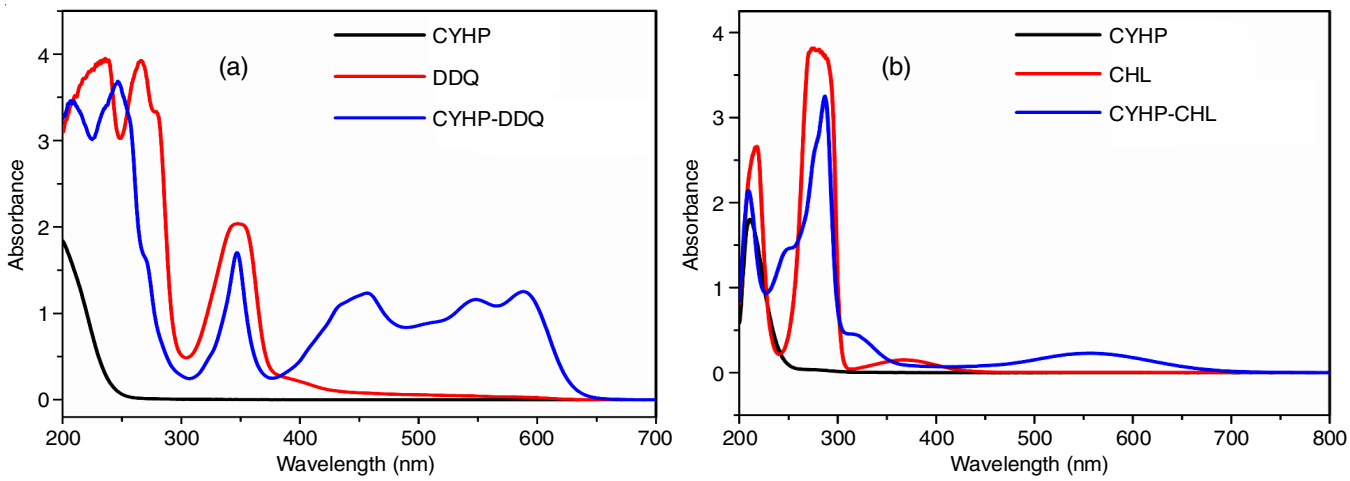

Fig. 1. Electronic absorption spectra of (a) CYHP, DDQ & [1-CYHP~DDQ] CT and (b) CYHP, CHL & [1-CYHP~CHL] CT complex in acetonitrile

absorption CT-bands. In the measured absorption spectra of CTC1 [(1-CYHP)(DDQ)], three charge transfer bands were observed at 588, 548 and 456 nm [24]. In case of CTC2 [(1-CYHP)(CHL)], the charge transfer band was observed at 557 nm, the formation of a coloured CHL radical anion is promoted by the donor 1-cyclohexylpiperazine (1-CYHP) with CHL. The development of CT-bands indicates that electrons are being transferred from donors to acceptors. The electronic transitions are from HOMO to LUMO. When acceptor DDQ and donor are mixed together, a reddish brown colour is visible, which is a feature of the CTC1 formation. Similarly, the acceptor CHL and donor are mixed together; a purple colour is visible, which is a feature of the CTC2 formation. The stable reddish brown colour of DDQ (**Scheme-I**) indicates the radical anion formed by electron transfer from 1-cyclohexylpiperazine to DDQ [25]. The radical anion is formed due to the contribution nature of the donor N-centre and DDQ's high electron affinity (1.9 eV). The existence of the DDQ radical anion may also be detected in the acrylonitrile polymerization process *i.e.*, conformation of radical anion. It was observed that the absorbances of CT complexes are stable for 1 h at 296 K [26].

Stoichiometry determination of CTC1 and CTC2: The molecular stoichiometries of CTCs were calculated using Job's continuous variation approach for CTC1 at 588 nm and CTC2 at 557 nm. In this method, the plot was drawn between absorption standards of designed [(1-CYHP)(DDQ)] complex and mole fraction corresponding to DDQ. From Fig. 2a, the maximum absorption peak at 0.5 mol indicating that 1:1 [(1-CYHP)-(DDQ)] complex was formed. Similarly, the extreme absorption peak at 0.5 mol indicates the 1:1 [(1-CYHP)(CHL)] CT complex has formed (Fig. 2b).

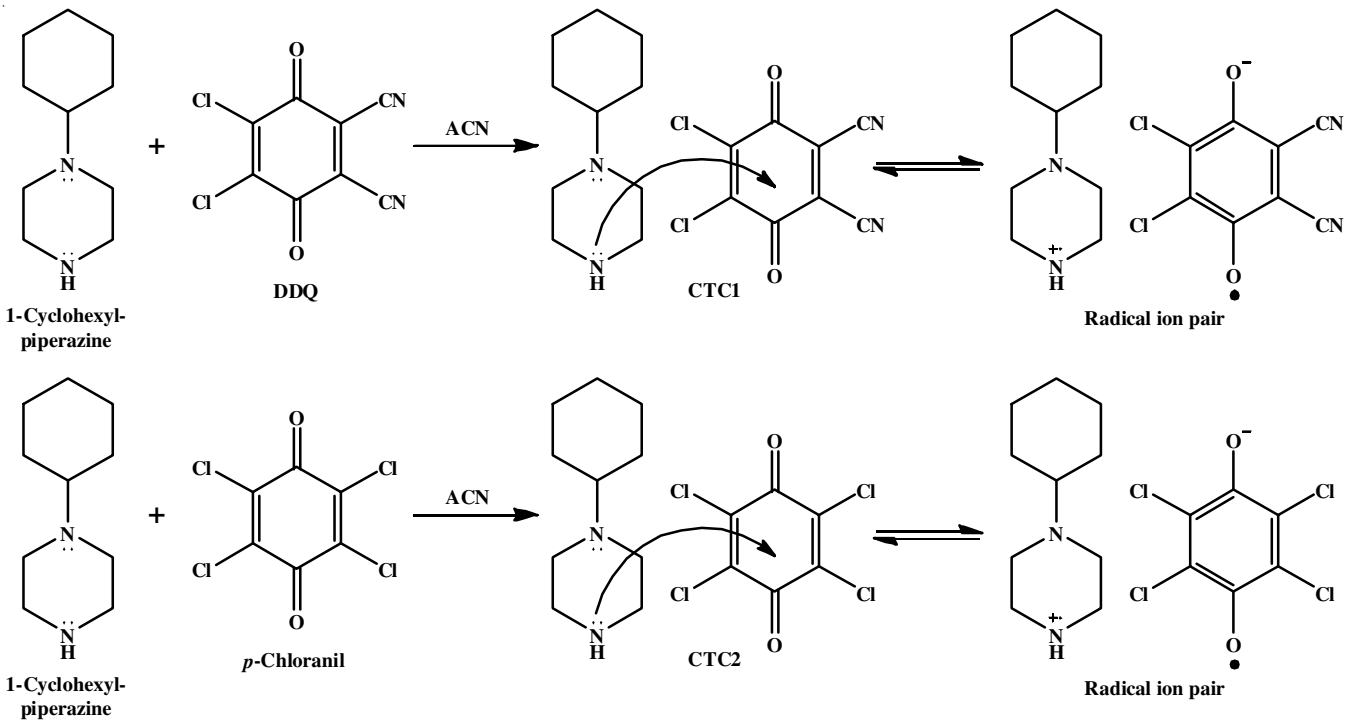

Scheme-I: Proposal CTC1 and CTC2 complexes formation mechanisms

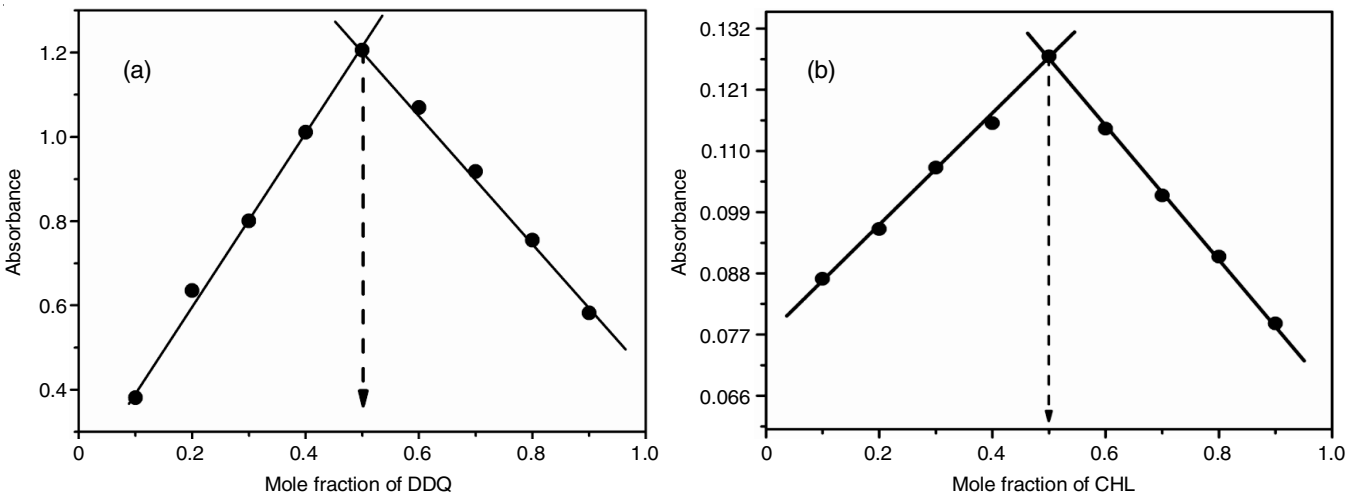

Fig. 2. Variation plot of the (a) [1-CYHP~DDQ] CT complex (CTC1) and (b) [1-CYHP~CHL] CT complex (CTC2)

Observation of the spectrophotometric titration plot revealed that two lines intersect at 1:1 ratio of donor (1-CYHP) to acceptors (DDQ and CHL), as clearly depicted in Fig. 3. Therefore, a 1:1 stoichiometry was confirmed for both CTCs, namely CTC1 and CTC2.

Stability (formation) constant (K_{CT}), molar extinction coefficient (ε_{CT}): The modified Benesi-Hildebrand equation [27] used for the constancy constant K_{CT} (L mol^{-1}) and the molar extinction coefficient ε_{CT} (L mol^{-1} cm^{-1}). At 588 nm, in CTC1 [(1-CYHP)(DDQ)] the acceptor concentration (5×10^{-4} M) was fixed, while the donor concentration (5×10^{-4} M to 1×10^{-4} M) was varied. In CTC2 [(1-CYHP)(CHL)], at 557 nm, the acceptor concentration was also fixed (5×10^{-4} M), but the donor concentration was changed from 5×10^{-4} M to 1×10^{-4} M. The absorbance of CT complexes rises at the same time, which is consistent with the existence of a persistent reddish brown colour for CTC1 and for CTC2 a purple colour at all doses of 1-cyclohexylpiperazine [28]. From the Benesi–Hildebrand equation (eqn. 1) at 1:1 ratio, the stability constant (K_{CT}) and molar extinction coefficient (ε_{CT}) were determined for both the CTC's.

$$\frac{C_a C_d}{A} = \frac{1}{K_{CT}\varepsilon} + \frac{(C_a - C_d)}{\varepsilon} \quad (1)$$

From Table-1, C_a represents the concentrations of DDQ and CHL acceptors and C_d is the concentration of donor 1-cyclohexylpiperazine; A denotes the CT-band absorbance at 588 nm for CTC1and 557 nm for CTC2. A graph of C_aC_d/A *versus* ($C_a + C_d$) gives a straight line, indicating that 1:1 CT complexes are formed. The straight line intercept and slope are equal to $1/K_{CT}$ and $1/\varepsilon_{CT}$ respectively. Furthermore, larger values of K_{CT} and ε_{CT} are attributed to acceptors electron affinity

TABLE-1
BENESI-HILDEBRAND DATA FOR 1:1 [(1-CYHP)(DDQ)] (CTC1) AND 1:1 [(1-CYHP)(CHL)] (CTC2) COMPLEXES AT DIFFERENT TEMPERATURES

C_a	C_d	A		$(C_aC_d/A) \times 10^{-7}$		$C_a + C_d$		$(C_a+C_d) \times 10^3$		$(C_aC_d/A) \times 10^6$	
		CTC1	CTC2	CTC1	CTC2	CTC1	CTC2	CTC1	CTC2	CTC1	CTC2
296 K											
0.0005	0.00010	0.445	0.076	1.12	6.58	0.00060	0.00060	0.60	0.60	0.1123	0.6578
0.0005	0.00015	0.587	0.112	1.28	6.70	0.00065	0.00065	0.65	0.65	0.1277	0.6690
0.0005	0.00020	0.714	0.141	1.40	7.09	0.00070	0.00070	0.70	0.70	0.1400	0.7092
0.0005	0.00025	0.858	0.164	1.46	7.62	0.00075	0.00075	0.75	0.75	0.1456	0.7621
0.0005	0.00030	0.976	0.194	1.54	7.73	0.00080	0.00080	0.80	0.80	0.1536	0.7731
0.0005	0.00035	1.145	0.206	1.53	8.50	0.00085	0.00085	0.85	0.85	0.1528	0.8495
0.0005	0.00040	1.171	0.232	1.71	8.62	0.00090	0.00090	0.90	0.90	0.1707	0.8620
0.0005	0.00045	1.268	0.244	1.77	9.22	0.00095	0.00095	0.95	0.95	0.1774	0.9221
0.0005	0.00050	1.313	0.261	1.90	9.58	0.00100	0.00100	1.00	1.00	0.1904	0.9578
301 K											
0.0005	0.00010	0.429	0.072	1.17	6.94	0.00060	0.00060	0.60	0.60	0.1165	0.6944
0.0005	0.00015	0.562	0.109	1.33	6.88	0.00065	0.00065	0.65	0.65	0.1334	0.6880
0.0005	0.00020	0.689	0.137	1.45	7.30	0.00070	0.00070	0.70	0.70	0.1451	0.7299
0.0005	0.00025	0.816	0.162	1.53	7.72	0.00075	0.00075	0.75	0.75	0.1531	0.7716
0.0005	0.00030	0.915	0.189	1.64	7.94	0.00080	0.00080	0.80	0.80	0.1639	0.7936
0.0005	0.00035	1.112	0.201	1.57	8.71	0.00085	0.00085	0.85	0.85	0.1573	0.8706
0.0005	0.00040	1.157	0.226	1.73	8.85	0.00090	0.00090	0.90	0.90	0.1728	0.8849
0.0005	0.00045	1.245	0.238	1.81	9.45	0.00095	0.00095	0.95	0.95	0.1807	0.9453
0.0005	0.00050	1.269	–	1.97	–	0.00100	–	1.00	–	0.1970	–
306 K											
0.0005	0.00010	0.412	0.069	1.21	7.25	0.00060	0.00060	0.60	0.60	0.1213	0.7246
0.0005	0.00015	0.543	0.106	1.38	7.08	0.00065	0.00065	0.65	0.65	0.1381	0.7075
0.0005	0.00020	0.668	0.132	1.50	7.58	0.00070	0.00070	0.70	0.70	0.1497	0.7575
0.0005	0.00025	0.789	0.158	1.58	7.91	0.00075	0.00075	0.75	0.75	0.1584	0.7911
0.0005	0.00030	0.876	0.184	1.71	8.15	0.00080	0.00080	0.80	0.80	0.1712	0.8152
0.0005	0.00035	0.995	0.193	1.76	9.07	0.00085	0.00085	0.85	0.85	0.1758	0.9067
0.0005	0.00040	1.129	0.218	1.77	9.17	0.00090	0.00090	0.90	0.90	0.1771	0.9174
0.0005	0.00045	1.225	0.232	1.84	9.70	0.00095	0.00095	0.95	0.95	0.1836	0.9698
0.0005	0.00050	1.258	0.249	1.99	1.00	0.00100	0.00100	1.00	1.00	0.1987	1.0040
311 K											
0.0005	0.00010	0.405	0.067	1.23	7.46	0.00060	0.00060	0.60	0.60	0.1234	0.7462
0.0005	0.00015	0.524	0.101	1.43	7.43	0.00065	0.00065	0.65	0.65	0.1431	0.7425
0.0005	0.00020	0.654	0.127	1.53	7.87	0.00070	0.00070	0.70	0.70	0.1529	0.7874
0.0005	0.00025	0.774	0.154	1.61	8.12	0.00075	0.00075	0.75	0.75	0.1614	0.8116
0.0005	0.00030	0.853	0.175	1.76	8.57	0.00080	0.00080	0.80	0.80	0.1758	0.8571
0.0005	0.00035	0.987	0.185	1.77	9.46	0.00085	0.00085	0.85	0.85	0.1773	0.9459
0.0005	0.00040	1.117	0.210	1.79	9.52	0.00090	0.00090	0.90	0.90	0.1790	0.9523
0.0005	0.00045	1.212	0.227	1.86	9.91	0.00095	0.00095	0.95	0.95	0.1856	0.9911
0.0005	0.00050	1.249	0.244	2.00	1.02	0.00100	0.00100	1.00	1.00	0.2001	1.0245

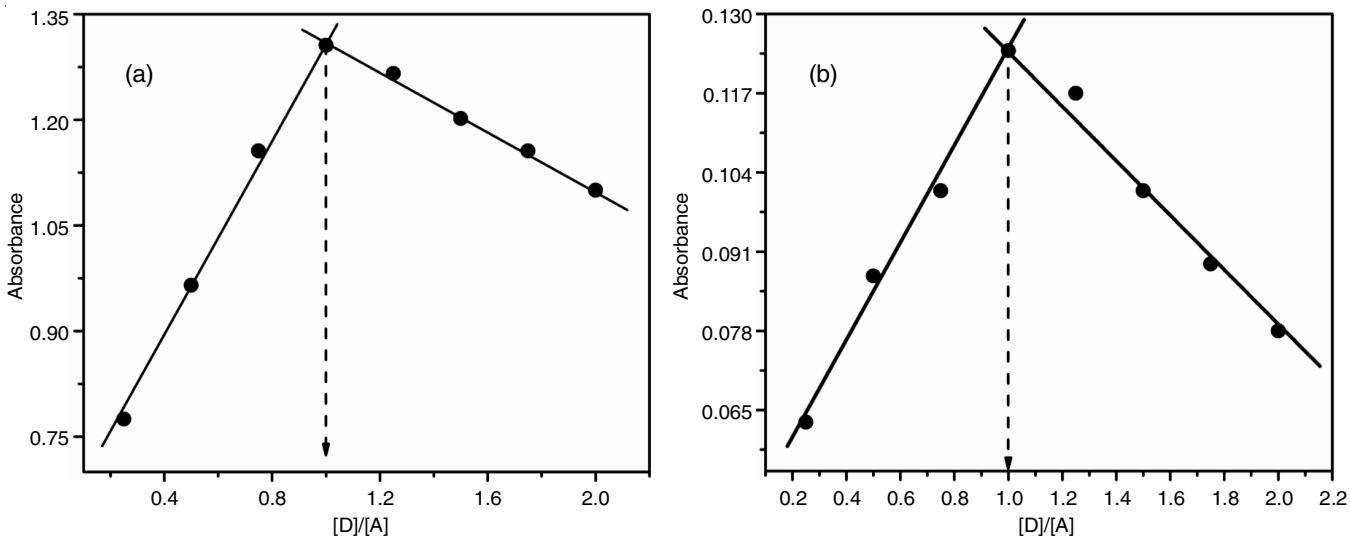

Fig. 3. Spectrophotometric plot of (a) [1-CYHP~DDQ] CT complex (CTC1) and (b) [1-CYHP~CHL] CT complex (CTC2)

and high donating nature of 1-cyclohexylpiperazine donor. The environment of the acceptor and the donor influence the stability constant.

Thermodynamic studies: In case of CTC1, the effect of temperature (Fig. 4) is displayed in Table-2. The absorbance of CTC1 found to decrease as the temperature rises, similarly the effect of temperature on CTC2 is shown in Table-2. For both CTCs the development/stability constant (K_{CT}), molar extinction coefficient (ε_{CT}) were computed at various temperatures between 296 and 311 K and the results are shown in Table-3. The $\Delta H°$ and $\Delta S°$ values were obtained from the following equation.

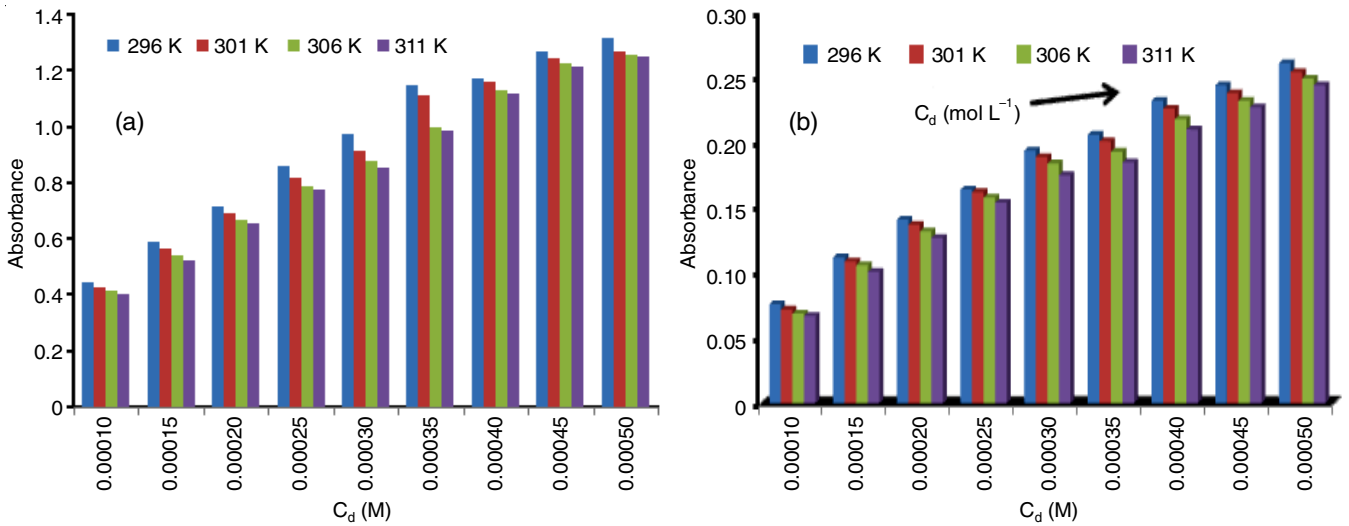

Fig. 4. Outcome of 1-CYHP concentration on the absorbance of CT complex with 5×10^{-4} mol L^{-1}; (a) DDQ and (b) CHL at diverse temperatures in acetonitrile

TABLE-2
OUTCOME OF 1-CYHP CONCENTRATION ON THE ABSORBANCE OF CTC1 AND CTC2 WITH 5×10^{-4} mol L^{-1} DDQ AND CHL AT 296-311 K

C_a	C_d	296 K		301 K		306 K		311 K	
		CTC1	CTC2	CTC1	CTC2	CTC1	CTC2	CTC1	CTC2
0.0005	0.00010	0.445	0.076	0.429	0.072	0.412	0.069	0.405	0.067
0.0005	0.00015	0.587	0.112	0.562	0.109	0.543	0.106	0.524	0.101
0.0005	0.00020	0.714	0.141	0.689	0.137	0.668	0.132	0.654	0.127
0.0005	0.00025	0.858	0.164	0.816	0.162	0.789	0.158	0.774	0.154
0.0005	0.00030	0.976	0.194	0.915	0.189	0.876	0.184	0.853	0.175
0.0005	0.00035	1.145	0.206	1.112	0.201	0.995	0.193	0.987	0.185
0.0005	0.00040	1.171	0.232	1.157	0.226	1.129	0.218	1.117	0.210
0.0005	0.00045	1.268	0.244	1.245	0.238	1.225	0.232	1.212	0.227
0.0005	0.00050	1.313	0.261	1.269	0.254	1.258	0.249	1.249	0.244

TABLE-3
STABILITY CONSTANTS, MOLAR EXTINCTION COEFFICIENTS AND OTHER PHYSICAL PARAMETERS OF THE FORMED (CTC1 AND CTC2) COMPLEXES

Complex	λ_{max} (nm)	Temp. (K)	$K_{CT} \times 10^3$ (L mol^{-1})	$\varepsilon \times 10^3$ (L mol^{-1} cm^{-1})	$-\Delta G°$ (KJ mol^{-1})	E_{CT} (eV)	I_D (eV)	$R_N \times 10$ (eV)	$-\Delta H$ (KJ mol^{-1})	ΔS (J K^{-1} mol^{-1})
CTC1	588	296	16.07	5.68	25.02	2.11	8.36	6.042	22.78	4.91
		301	9.66	5.74	23.34					
		306	6.88	5.81	22.11					
		311	5.21	5.98	21.06					
CTC2	557	296	4.63	1.267	20.771	2.23	7.73	6.37	19.37	4.56
		301	4.03	1.278	20.776					
		306	3.55	1.283	20.805					
		311	3.05	1.291	21.318					

$$\ln K_{CT} = \frac{-\Delta H°}{RT} + \frac{\Delta S°}{R} \quad (3)$$

Entropy and enthalpy variation during the formation of the CT complexes are represented by $\Delta S°$ and $\Delta H°$. Fig. 5 shows straight line is generated by plotting ln K_{CT} *versus* 1000/T. The slope of the linear fitted line on the graph corresponds to (-$\Delta H°$/R), while the intercept corresponds to ($\Delta S°$/R). The values of $\Delta H°$ and $\Delta S°$ for both CTCs were calculated and are presented in Table-3. From the van't Hoff plot, the positive slopes indicates the CTC1 and CTC2 formed *via* exothermic.

Calculation of donor~acceptor interaction energy (E_{CT}): Eqn. 4 is used to calculate the donor~acceptor interaction energy (E_{CT}) [29] of [(1-CYHP)(DDQ)] and [(1-CYHP)(CHL)] complexes.

$$E_{CT} = \frac{1243.667}{\lambda_{CT}} \quad (4)$$

λ_{CT} denotes the wavelength of the CT- band of complex. The K_{CT}, ε_{CT} and E_{CT} values support the formation of stable complexes.

Free energy ($\Delta G°$) calculation: CT complexes free energy change, $\Delta G°$ (KJ mol^{-1}) was calculated using the following equation [30]:

$$\Delta G° = -RT \ln K_{CT} \quad (5)$$

where, $\Delta G°$ = complex's standard Gibbs free energy change, R = universal gas constant (8.314 J mol^{-1} K^{-1}), T = temperature in Kelvin, K_{CT} = donor–acceptor complex formation constant (L mol^{-1}).

In Table-3, the complex $\Delta G°$ values are also presented. The signs $\Delta H°$ and $\Delta G°$ imply the CT complexes developed exothermically and spontaneously.

Ionization potential (I_D) of donor in CTCs: Ionization potential (I_D) of the donor (1-CYHP) in CTC1 and CTC2 were calculated based on an empirical relationship proposed by Aloisi & Piganataro [31] and Refat *et al.* [32]:

$$I_D = 5.76 + 1.52 \times 10^{-4} \nu_{CTC1} \quad (6)$$

$$I_D = 5.00 + 1.53 \times 10^{-4} \nu_{CTC2} \quad (7)$$

where I_D = ionization potential of is the donor molecule and ν_{CT} = CT band's wavenumber in cm^{-1}. The ionization potential of donor is the amount of energy mandatory to eject an electron (-ve charge) from HOMO, which determines the electron-contributing character of donor.

Scheming of resonance energy (R_N): Brieglb & Czekalla [33] hypothetically derived eqn. 8 for calculating resonance energy (R_N) in both produced CTCs.

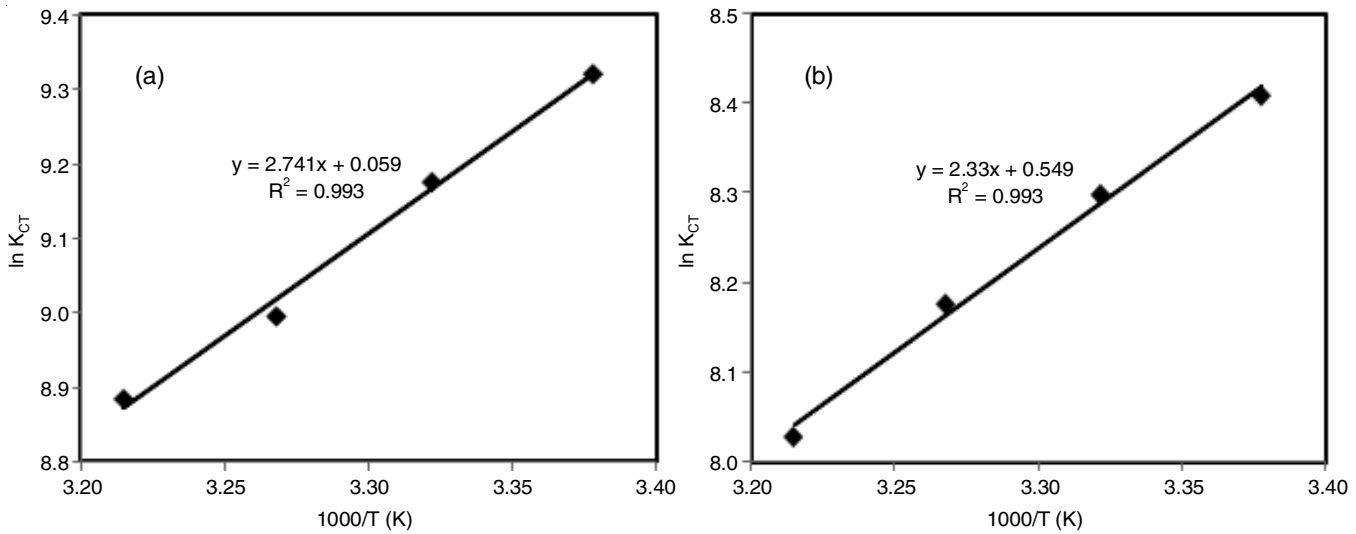

Fig. 5. van't Hoff plot for (a) [1-CYHP~DDQ] CTC1 and (b) [1-CYHP~CHL] CTC2

$$\varepsilon_{CT} = \frac{7.7\times10^{-4}}{\left[h\nu_{CT}/|R_N|-3.5\right]} \quad (8)$$

where ν_{CT} = frequency of CT peak; R_N = resonance energy of the complexes; ε_{CT} = molar extinction coefficient at the CT band's greatest absorption.

Energy (E_{CT}), the donor's ionization potential (I_D) and the acceptor's electron affinity (EA) were used to determine the dissociation energy (W) of CT complexes using eqn. 9:

$$W = I_D - EA - E_{CT} \quad (9)$$

FT-IR spectral studies: The FT-IR spectral analysis of both CT complexes (CTC1 and CTC2) were observed in the range of 4000-500 cm^{-1}. The spectra results of donor (1-CYHP) acceptors (DDQ and CHL), CTC1 (1-CYHP~DDQ) and CTC2 (1-CYHP~CHL) are shown in Fig. 6 and the key vibrations are shown in Table-4.

The formation of CT complexes is due to transfer of electrons from a donor (1-cyclohexylpiperazine) to acceptors (DDQ and CHL). In case of DDQ in CTC1, the wavenumber of ν(C≡N) upon complexation moved to lower wavenumber 2206.06 cm^{-1} as compared to 2227.56 cm^{-1} of free state, also ν(C=O) wavenumber 1675.90 cm^{-1} of DDQ in free state changed to 1636.22 cm^{-1} upon CT-complex formation. The electron withdrawing nature and the conjugated system of DDQ is responsible in reduction in (C≡N) bond length and vibration wavenumber through the establishment of the CTC. Subsequently, the NH group of 1-cyclohexylpiperazine illustrate in the evolution of CT-complex with DDQ, moreover in CT-complex, the acceptor's (C–Cl) is moved towards lower frequency in the second instance. In CTC2 (1-CYHP~CHL), the ν(C=O) of CHL in free state wavenumber 1680.31 cm^{-1} was moved towards lowered value of 1655.77 cm^{-1} upon complexation. The IR spectra of donor molecule was shifted to higher values in their corresponding complexes *i.e.*, from 3422.48 cm^{-1} to 3445.84 cm^{-1} in CTC1 and from 3422.48 cm^{-1} to 3450.89 cm^{-1} in CTC2.

NMR spectral studies: The ^1H NMR spectra of CTC1 (1-CYHP~DDQ) and CTC2 (1-CYHP~CHL) were recorded in $CDCl_3$ and are shown in Fig. 7. Because of the de-shielding of protons increases at the time of contact with the acceptor, the ^1H NMR spectrum of CTC1 and CTC2 complexes signals are moved downfield (decreasing δ value) owing to protons of the donor. The base for the above results are due to the electron transfer process from donor (1-CYHP) to acceptors (DDQ and

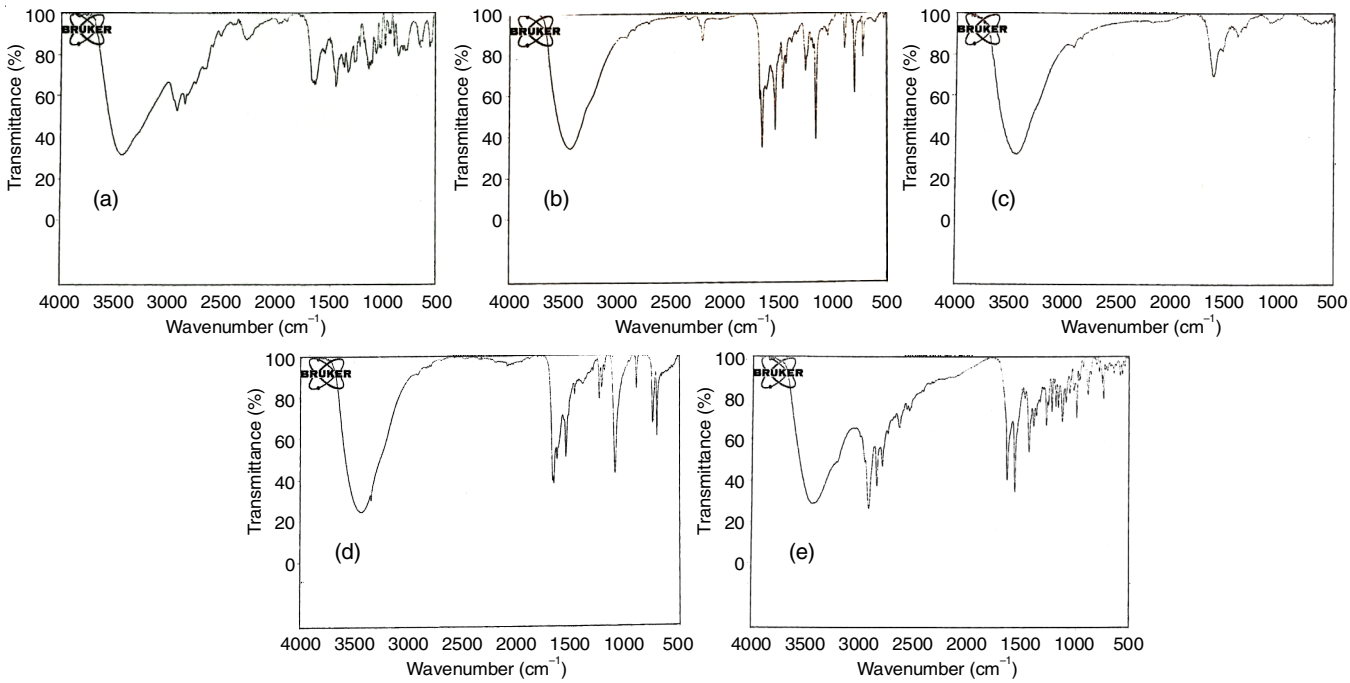

Fig. 6. FTIR spectra of (a) donor (1-CYHP); (b) acceptor (DDQ), (c) [1-CYHP + DDQ] CT complex, (d) acceptor (CHL) and (e) [(1-CYHP+ CHL)] CT complex

TABLE-4
CHARACTERISTIC INFRARED FREQUENCIES AND BAND TASKS FOR DONOR (1-CYHP), ACCEPTORS (DDQ, CHL) AND CT COMPLEXES (CTC1 AND CTC2)

1-CYHP	DDQ	CTC1	CHL	CTC2	Assignments
	2227.56 cm^{-1}	2206.06 cm^{-1}			ν(C≡N)
3422.48 cm^{-1}	1675.90 cm^{-1}	1636.22 cm^{-1}			ν(C=O)
		3445.84 cm^{-1}			ν(N-H)
			1680.31 cm^{-1}	1655.77 cm^{-1}	ν(C=O)
3422.48 cm^{-1}			753.17 cm^{-1}	751.26 cm^{-1}	ν(C-Cl)
				3450.89 cm^{-1}	ν(N-H)

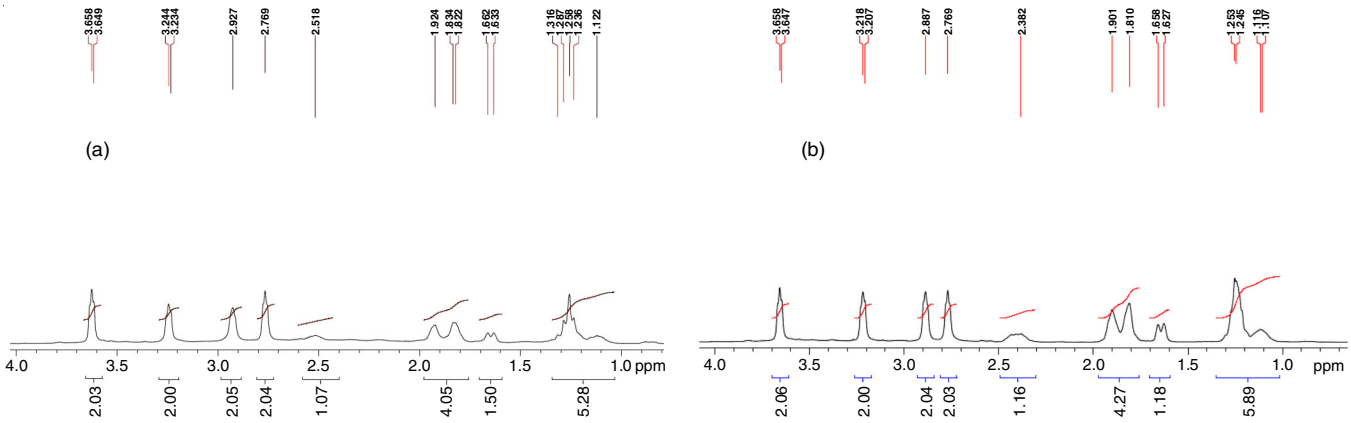

Fig. 7. ^{1}H NMR spectra of (a) CTC1 and (b) CTC2 in $CDCl_3$

CHL), it was observed that the proton shift in CTC1 is more (higher δ ppm) when compared to CTC2.

CT-DNA binding studies: The CT complexes binding interaction with CT-DNA is defined by changes in wavelength and absorbance when CT-DNA solution is added towards complexes. In this work, the binding affinity was determined by measuring the change in absorbance of CT complexes as the concentration of CT-DNA was increased, while keeping the concentration of CT complexes constant. The CT-complexes with CT-DNA have slight red shift and are hypochromic in their electronic absorption spectrum, indicating that CTCs bind with CT-DNA bind in intercalation mode. These absorption spectra are shown in Fig. 8.

When the CT-DNA to CTCs concentration ratio was increased, a reduction in absorbance was detected and the wavelength shifted towards longer wavelengths (red shift) in these spectra due to strong binding between the aromatic chromospheres of the CT-complexes and adjacent base pairs of CT-DNA [34]. DNA intercalation is possible due to the aromatic rings and π-system of CT complexes. The magnitude of the hypochromism generally corresponds to the degree of intercalative binding, implying that CT-complexes have an intercalative interaction with the DNA helix. The Wolfe-Shimmer equation (eqn. 10) was used to investigate the absorption data and calculated the intrinsic binding constant (K_b) [35,36].

$$\frac{[DNA]}{(\varepsilon_a - \varepsilon_f)} = \frac{[DNA]}{(\varepsilon_b - \varepsilon_f)} + \frac{1}{K_b(\varepsilon_b - \varepsilon_f)} \quad (10)$$

where K_b = binding constant, [DNA] = concentration of DNA in the base pairs, ε_a = apparent coefficient equal to A_{obs}/[CT-complex], ε_f, ε_b = extinction coefficients of the free and fully bound to DNA, respectively.

From the Wolfe-Shimmer equation, a plot of [DNA]/(ε_a – ε_f) *versus* [DNA], the binding constant (K_b) were calculated from the ratio of slope to the intercept. The CTCs binding affinity is directly related to binding constant. The high (K_b) binding constant value indicates that the CT-complexes have a high affinity for binding. CTC1 shows good binding affinity ($K_b = 3.6 \times 10^3\ M^{-1}$) when compared to CTC2 binding affinity ($2.79 \times 10^2\ M^{-1}$).

Computational analysis

Bond lengths and bond angles: Density functional theory (DFT) was used to conduct the theoretical research. This model

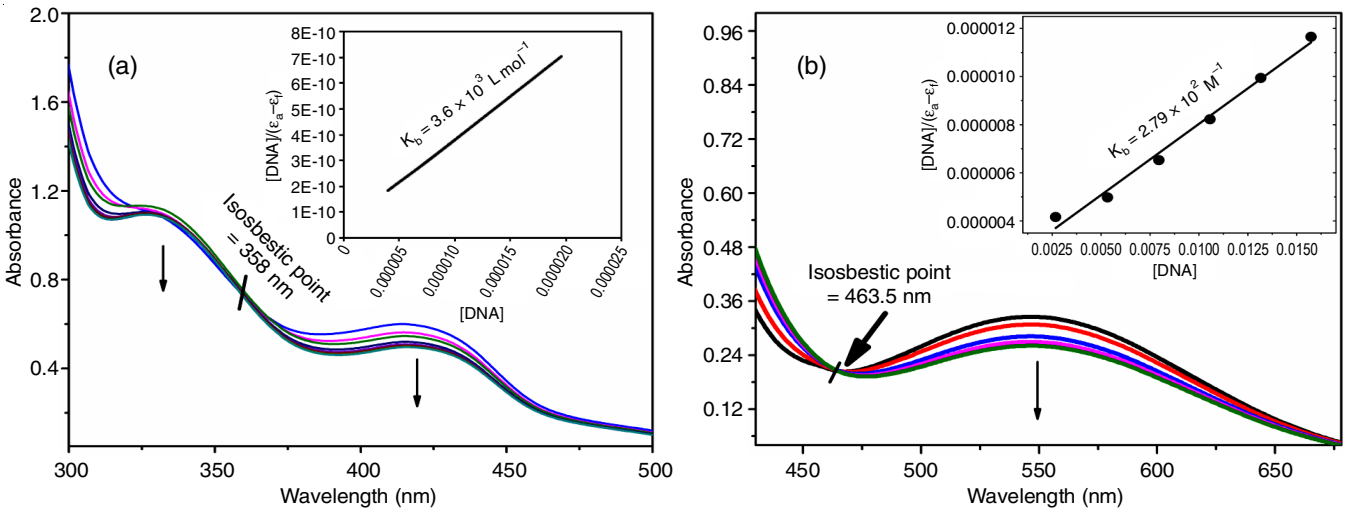

Fig. 8. (a) CTC1 and (b) CTC2 electronic absorption spectra with growing CT-DNA concentrations from 0 to 10 μM and constant CTC1 complex concentrations. Arrows (↓) indicate changes in absorption intensity upon increasing DNA concentration. Insets depict linear plots used for calculating the intrinsic binding constant

has been frequently applied for analyzing optimization results and determining electronic characteristics [37]. The improved geometries of 1-cyclohexylpiperazine, DDQ, CHL and a 1:1 ratio of (1-CYHP~DDQ) CT-complex and (1-CYHP~CHL) complex were analyzed. The bond lengths of 1-cyclohexylpiperazine, CHL, DDQ, [(1-CYHP)(DDQ)] CTC1 and [(1-CYHP)-(CHL)] CTC2 complexes were computed using these structures and the results are given in Table-5. In CTC1, the C–O bond length in DDQ [C(1)-O(7)] and [C(4)-O(8)] improved to 1.259 Å and 1.263 Å, respectively, compared to 1.2401 Å in free DDQ. The bond length of DDQ [C(11)-N(13) and C(12)-N(14)] of the cyano group in CTC1 extended to 1.1754 Å and 1.1751 Å when compared to 1.1732 Å of free DDQ. It is possible to deduce from the above observations that the cyano group possesses a double bond rather than a triple bond, suggesting the formation of a DDQ radical anion in the CT complex. When the length of bonds of DDQ [C(6)-Cl(9) and C(5)-Cl-(10)] were examined, the bond length of (C–Cl) CTC1 rose to 1.7922 Å and 1.8033 Å, respectively, contrast to 1.7807 Å of free DDQ. The bond lengths of carbon and oxygen [C(5)-O(11) and C(2)-O(12)] in CHL of CT-complex increased to 1.2617 Å and 1.2557 Å, respectively when compared with 1.2381 Å as compared to free CHL, also the C and Cl bond lengths of CTC2 in CHL [C(3)-Cl(8), C(4)-Cl(7), C(6)-Cl(10), C(1)-Cl(9)] increased to 1.7995 Å, 1.8017 Å, 1.8122 Å and 1.8026 Å, respectively when compared to1.7832 Å as compared to free CHL. The above results point to the formation of a CHL radical anion in the CT complex. The electrons migrate to the DDQ and CHL components of the CT-complex, where they generate the resonant configurations. Upon complexation, the bond length of the donor moiety is observed to decrease, as illustrated in **Scheme-I**. The establishment of CT-complexes (CTC1 and CTC2) is additionally verified by the changes observed in the bond angles of complexes as compared to free donor and acceptors as shown in Tables 6 and 7. In CTC1(1-CYHP~DDQ) the bond angle of DDQ free radical anion of C(2)-C(1)-O(7) is increased to 122.079º from 120.240º of free DDQ, similarly the bond angle of C(3)-C(4)-O(8) is increased to 121.754° from 120.240° of free DDQ. The bond angle of C(3)-C(2)-C(11) decreased to 120.891º from 122.408º as compared to free DDQ. In CTC2 [(1-CYHP)(CHL)], the bond angles of CHL [C(6)-C(5)-O(11), C(1)-C(2)-O(12)] are increased (from 121.767º to 123.471º) and (121.767º to 123.119º) as compared to free CHL. In case of donor 1-CHYP, the bond angle of [C(24)-N(19)-C(27)] in CTC1 increased to 118.20º from 112.26º as compared to free 1-CYHP, also the bond angle of C(21)-N(18)-C(30) in CTC1 increased to 117.06º from 112.07º. In CTC2, similar results are observed.

Mulliken atomic charges: In charge transfer (CT) complexes, estimating Mulliken atomic charges is important for quantum mechanical calculations on molecular systems [38]. Table-8 shows the Mulliken atomic charges that have been determined. Mulliken electronic charges on N(l3) and N(l4) increased from -0.157, -0.157 to -0.212 and -0.223 au, respectively. Also, on C(1), C(2), Cl(9) and O(7) atoms of DDQ were found to be 0.331, 0.151, 0.246 and -0.3145 au, respectively and on complexation negative charges increased to C(1) = 0.291, C(2) = 0.105, Cl(9) = 0.163 and O(7) = -0.419 au, respectively and similarly the charges on O(11) and O(12) of CHL increased from -0.332 and -0.332 to -0.454 and -0.416 au, respectively.

TABLE-5
GROUND STATE (DFT) GEOMETRIC BOND LENGTH VALUES (Å) OF DDQ, CHL, 1-CYHP AND CT COMPLEXES

Parameter	1-CYHP	CHL	1-CYHP-CHL	Parameter	DDQ	1-CYHP-DDQ
C(1)-C(4)	1.540		1.540			1.552
C(4)-C(7)	1.551		1.552			1.553
C(7)-C(10)	1.553		1.554			1.544
C(10)-C(12)	1.549		1.543			1.551
C(12)-C(15)	1.552		1.554			1.552
C(1)-C(15)	1.554		1.554			1.540
C(10)-N(18)	1.482		1.484			1.492
N(18)-C(21)	1.474		1.400			1.390
C(21)-C(24)	1.540		1.355			1.360
N(19)-C(24)	1.472		1.399			1.393
N(19)-H(20)	1.018		1.008			1.008
N(19)-C(27)	1.472		1.402			1.395
C(27)-C(30)	1.540		1.354			1.358
N(18)-C(30)	1.474		1.401			1.399
C(1)-C(2)		1.4892	1.4661	C(1)-C(2)	1.497	1.4666
C(2)-C(3)		1.4892	1.4786	C(1)-O(7)	1.2401	1.2599
C(3)-C(4)		1.3575	1.3567	C(4)-O(8)	1.2401	1.2633
C(4)-C(5)		1.4892	1.3567	C(11)-N(13)	1.1732	1.1754
C(5)-C(6)		1.4892	1.4664	C(12)-N(14)	1.1732	1.1751
C(1)-C(6)		1.3472	1.3626			
C(2)-O(12)		1.2381	1.2552			
C(5)-O(11)		1.2381	1.2617			
C(1)-Cl(9)		1.7832	1.8026			
C(6)-Cl(10)		1.7832	1.8122			
C(3)-Cl(8)		1.7832	1.7995			
C(4)-Cl(7)		1.7832	1.8017			

TABLE-6
OPTIMIZED (DFT/6-31G) BOND ANGLE (°) VALUES FOR DDQ, 1-CYHP AND CTC

Parameter	1-CYHP	1-CYHP/CTC	Parameter	DDQ	DDQ/CTC
C(1)-C(4)-C(7)	111.149	112.354	C(1)-C(2)-C(3)	121.002	122.023
C(1)-C(15)-C(12)	112.308	111.516	C(2)-C(3)-C(4)	121.002	121.294
C(4)-C(7)-C(10)	112.578	110.350	C(3)-C(4)-C(5)	117.353	115.827
C(10)-C(12) -C(15)	110.816	111.517	C(4)-C5)-C(6)	121.644	122.302
C(4)-C(1)-C(15)	111.078	110.979	C(6)-C(1)-C(2)	117.353	115.486
C(7)-C(10)-N(18)	111.031	111.292	C(5)-C(6)-C(1)	121.644	122.408
C(12)-C(10)-N(18)	115.585	113.021	C(1)-C(2)-C(11)	116.589	116.957
C(10)-N(18)-C(21)	115.440	120.218	C(2)-C(3)-C(12)	122.408	121.749
C(10)-N(18)-C(30)	116.854	122.174	C(4)-C(3)-C(12)	116.589	116.956
N(18)-C(21)-C(24)	109.765	121.934	C(3)-C(2)-C(11)	122.408	120.891
C(21)-C(24)-N(19)	112.792	120.478	C(2)-C(1)-O(7)	120.240	122.079
C(24)-N(19)-C(27)	112.269	118.202	C(6)-C(1)-O(7)	122.405	122.433
C(24)-N(19)-H(20)	112.340	120.852	C(1)-C(6)-Cl(9)	115.427	115.362
C(30)-C(27)-N(19)	112.697	120.730	C(5)-C(6)-Cl(9)	122.928	122.170
C(27)-N(19)-H(20)	112.300	120.922	C(6)-C(5)-Cl(10)	122.928	122.182
C(21)-N(18)-C(30)	112.074	117.063	C(4)-C(5)-Cl(10)	115.427	115.515
N(18)-C(30)- C(27)	109.612	121.552	C(5)-C(4)-O(8)	120.240	121.397
C(7)-C(10)-C(12)	110.401	111.435	C(3)-C(4)-O(8)	120.240	121.754

TABLE-7
OPTIMIZED (DFT/6-31G) BOND ANGLE (°) VALUES FOR 1-CYHP, CHL AND CTC

Parameter	1-CYHP	1-CYHP/CTC	Parameter	CHL	CHL/CTC
C(1)-C(4)-C(7)	111.149	111.410	C(1)-C(2)-C(3)	116.465	114.522
C(1)-C(15)-C(12)	112.308	112.503	C(2)-C(3)-C(4)	121.767	122.710
C(4)-C(7)-C(10)	112.578	111.917	C(3)-C(4)-C(5)	121.767	122.594
C(10)-C(12)-C(15)	110.816	110.196	C(4)-C5)-C(6)	116.465	114.498
C(4)-C(1)-C(15)	111.078	111.156	C(6)-C(1)-C(2)	121.767	122.344
C(7)-C(10)-N(18)	111.031	111.631	C(5)-C(6)-C(1)	121.767	123.080
C(12)-C(10)-N(18)	115.585	112.730	C(1)-C(2)-O(12)	121.7673	123.1191
C(10)-N(18)-C(21)	115.440	121.033	C(2)-C(1)-Cl(9)	115.272	115.404
C(10)-N(18)-C(30)	116.854	120.948	C(2)-C(3)-Cl(8)	115.272	115.008
N(18)-C(21)-C(24)	109.765	121.249	C(4)-C(3)-Cl(8)	122.959	122.274
C(21)-C(24)-N(19)	112.792	119.847	C(3)-C(4)-Cl(7)	122.959	122.296
C(24)-N(19)-C(27)	112.269	119.606	C(5)-C(4)-Cl(7)	115.272	115.072
C(24)-N(19)-H(20)	112.340	120.277	C(4)-C(5)-O(11)	121.767	121.990
C(30)-C(27)-N(19)	112.697	119.505	C(6)-C(5)-O(11)	121.767	123.471
C(27)-N(19)-H(20)	112.300	119.368	C(5)-C(6)-Cl(10)	115.272	115.154
C(21)-N(18)-C(30)	112.074	118.012	C(1)-C(6)-Cl(10)	122.960	121.759
N(18)-C(30)- C(27)	109.612	121.552	C(6)-C(1)-Cl(9)	122.960	122.227
C(7)-C(10)-C(12)	110.401	111.030	C(3)-C(2)-O(12)	121.767	122.356

TABLE-8
MULLIKEN ATOMIC CHARGE VALUES FOR 1-CYHP, CHL, DDQ AND CT COMPLEXES

Atom	1-CYHP	1-CYHP/ CTC1	1-CYHP/ CTC2	Atom	CHL	CHL/ CTC1	Atom	DDQ	DDQ/ CTC2
C(1)	-0.247	-0.255	-0.256	C(1)	-0.260	-0.277	C(1)	0.331	0.291
C(4)	-0.252	-0.255	-0.252	C(2)	0.393	0.369	C(2)	0.151	0.105
C(7)	-0.232	-0.249	-0.242	C(3)	-0.260	-0.268	C(3)	0.151	0.107
C(10)	0.0454	0.019	0.019	C(4)	-0.260	-0.251	C(4)	0.331	0.323
C(12)	-0.255	-0.245	-0.254	C(5)	0.393	0.404	C(5)	-0.263	-0.255
C(15)	-0.249	-0.253	-0.259	C(6)	-0.260	-0.277	C(6)	-0.263	-0.275
C(21)	-0.093	0.128	0.129	Cl(7)	0.229	0.142	O (7)	-0.314	-0.419
C(24)	-0.123	0.084	0.098	Cl(8)	0.229	0.151	O(8)	-0.314	-0.445
C(27)	-0.122	0.103	0.102	Cl(9)	0.229	0.145	Cl(9)	0.246	0.163
C(30)	-0.099	0.131	0.127	Cl(10)	0.229	0.129	Cl(10)	0.246	0.147
N(18)	-0.617	-0.473	-0.586	O(11)	-0.332	-0.454	N(13)	-0.157	-0.212
N(19)	-0.688	-0.537	-0.538	O(12)	-0.332	-0.416	N(14)	-0.157	-0.223
H(20)	0.266	0.355	0.367						

In case of 1-CHYP charges on N(18) and N(19) found to be -0.617 a.u and -0.688, respectively, which upon complexation decreases with DDQ and CHL. Based on the above observations, it was found that there is a significant increase of negative charge on the acceptor atoms (DDQ and CHL) and decrease of charge on the donor atoms. This shows that there has been a significant quantity of electronic charge moved from 1-CHYP to DDQ and CHL during complexation.

Molecular electrostatic potential surfaces: The electrostatic potential surface maps were created using the DFT approach, with a basis set of 6–31 G utilized for geometry optimization. The charge change of CT complexes was assessed using molecular electrostatic potential [39]. Fig. 9 displays the MEP surface maps, with acceptor DDQ's MEP confined by a positive charge (0.0065 a.u.) on the DDQ moiety's centre. The cyano group and the O-carbonyl group in DDQ have a negative charge (-0.0595 au, -0.0622 au). In CHL, the positive potential (blue) with high surface value (0.0475 au) was confined to centre of the CHL moiety, whereas a negative potential (red) was observed surrounding the carbonyl group atoms (-0.0353 a.u. and -0.0349 a.u.). Because of the presence of lone pairs of the N-atomic groups, the negative charges (-0.0566 a.u., -0.0420 a.u.) are associated with the donor 1-cyclohexylpiperazine. The central positive value of DDQ raised to 0.0628 a.u. after 1-cyclohexylpiperazine interacted with it, while the potentials of the N-atoms of cyano groups and the O-atoms of carbonyl groups increase to -0.03867 a.u, -0.03867 a.u and -0.2796 a.u, -0.2769 a.u, respectively. Upon formation of the CT complex, the centre of the ring potential fell to 0.05 a.u, whereas the potential of the nitrogen atoms 1-cyclohexylpiperazine increased from -0.0566 and -0.04202 to 0.0766 and 0.0551 au. In CTC2, the CHL centre surface value was lowered to 0.017 a.u. The 'O' atoms of carbonyl groups potential values (-0.066 and -0.057 a.u) and the nitrogen atoms in 1-cyclohexylpiperazine potential (0.053 and 0.049 a.u) increased as a result of the formation of the CT-complex (Fig. 9). According to these observations, charge density travels from N-atoms of 1-cyclohexylpiperazine to C=O groups of CHL and DDQ. It backs up the hypothesis that DDQ and CHL are frequently utilized to frame CT complexes containing noble electron acceptors of various types.

Frontier molecular orbital (HOMO-LUMO) energies calculations for CT complexes: The HOMO~LUMO energies

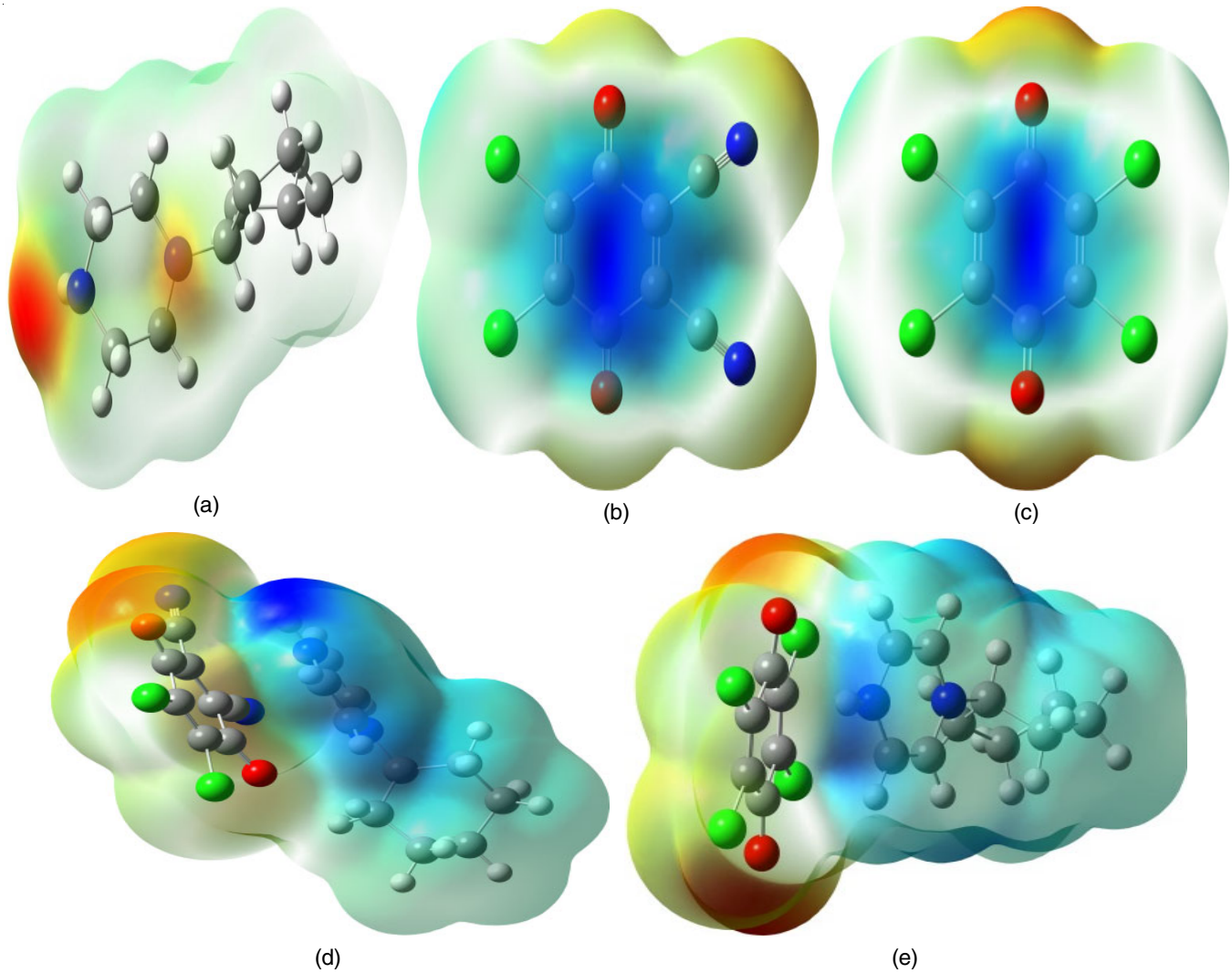

Fig. 9. Molecular electrostatic potential surface maps for (a) 1-CYHP, (b) DDQ, (c) CHL, (d) 1-CYHP~DDQ, CTC1 and (e) 1-CYHP~CHL, CTC2 in ground state (gas phase)

[40-43] in the ground state were calculated using a DFT approach. The HOMO and lowest vacant molecular orbital energies are used to compute the electron cloud distribution of CTC1 and CTC2, as illustrated in Fig. 10. In CTC1, the HOMO, HOMO-1 and HOMO-2 are localized on 1-cyclohexylpiperazine, but LUMOs were primarily found on the DDQ moiety. For CTC2, the HOMO, HOMO-1 is exclusively on 1-cyclohexylpiperazine LUMOs, on the other hand, are mostly found on the CHL moiety. From Table-9, it is found that [(1-CYHP)-(DDQ)] CT-complex LUMO energy values (-0.1240 Ha) is similar to the LUMO energy of DDQ (-0.2001 Ha), on the other hand HOMO energy values of [(1-CYHP)(DDQ)] CT complex's (-0.1978 Ha) is close to 1-CYHP HOMO energy value (-0.1946 Ha). Also the [(1-CYHP)(CHL)] CT complex's LUMO energy value (-0.1145 Ha) is similar to the LUMO energy of CHL (-0.0754 Ha), on the other hand HOMO energy values of [(1-CYHP)(CHL)] CT complex's (-0.1958 Ha) is close to 1-CYHP HOMO energy value (-0.1946 Ha). Thus, the patterns observed in the CTC1 and CTC2 structures restrict the localization of border molecular orbitals, similar to the electron movement complex structure as stated earlier.

Reactivity descriptors from computational studies: The reactivity parameters [44] of donor and acceptors and charge transfer complexes CTC1 [(1-CYHP)(DDQ)] and CTC2 [(1-CYHP)(CHL)] are mentioned in Table-10.

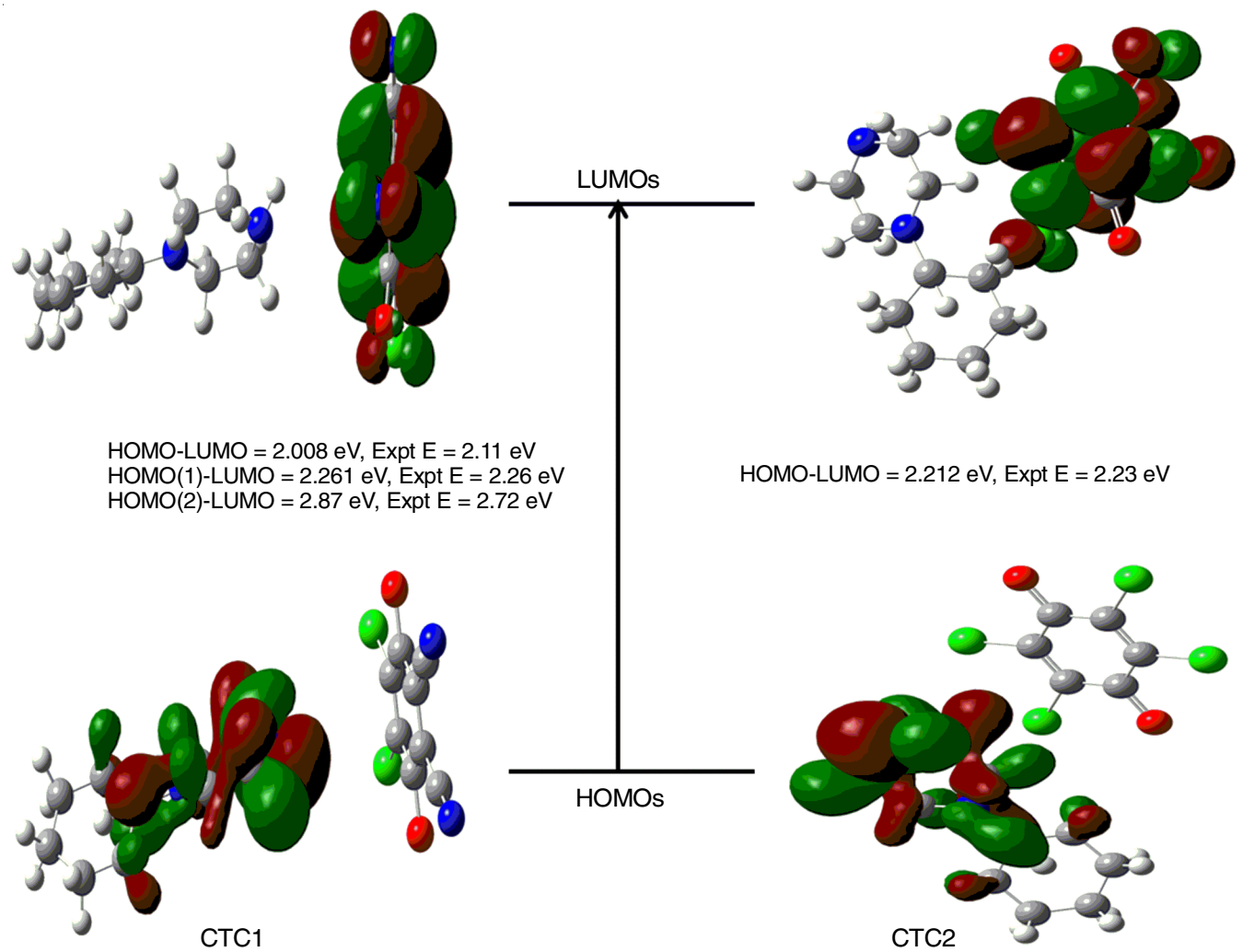

Fig. 10.

TABLE-9
HOMO–LUMO ENERGY VALUES FOR CHL, DDQ AND 1-CYHP AND CT COMPLEX IN OPTIMIZED FORM

Orbital energy (Hatree)											
MO	1-CYHP	CHL	DDQ	1-CYHP-CHL	1-CYHP-DDQ	MO	1-CYHP	CHL	DDQ	1-CYHP-CHL	1-CYHP-DDQ
HOMO	-0.1946	-0.3007	-0.3192	-0.1958	-0.1978	LUMO	0.0754	-0.1762	-0.2001	-0.1145	-0.1240
HOMO-1	-0.1993	-0.3176	-0.3348	-0.2052	-0.2071	LUMO+1	0.0890	-0.0676	-0.1214	-0.0467	-0.0749
HOMO-2	-0.2238	-0.3177	-0.3419	-0.2275	-0.2298	LUMO+2	0.0953	-0.0669	-0.0693	-0.0379	-0.0660
HOMO-3	-0.2611	-0.3284	-0.3433	-0.2409	-0.2413	LUMO+3	0.1118	-0.0402	-0.0679	-0.0250	-0.0346
HOMO-4	-0.2772	-0.3443	-0.3574	-0.2535	-0.2563	LUMO+4	0.1228	-0.0380	-0.0335	-0.0041	-0.0125

TABLE-10
ELECTRONIC REACTIVITY DESCRIPTORS OF THE DDQ AND 1-CYHP AND CTC1 [(1-CYHP) (DDQ)] AND CTC2 [(1-CYHP) (CHL)]

Parameter	1-CYHP	DDQ	CHL	[(1-CYHP) (DDQ	[(1-CYHP) (CHL)]
E_{HOMO} (eV)	-5.2763	-8.6547	-8.1531	-5.3631	-5.3089
E_{LUMO} (eV)	2.0443	-5.4255	-4.777	-3.3621	-3.1045
I	5.2763	8.6547	8.1531	5.3631	5.3089
A	-2.0443	5.4255	4.777	3.3621	3.1045
η	3.6598	1.6146	1.688	1.0005	1.1002
μ	-1.616	-7.0401	-6.4650	-4.3626	-4.2067
ω	0.356	15.349	12.3805	9.5113	8.0277
σ	0.2732	0.6139	0.5924	0.9995	0.9072

1 eV = 96.485 kJ mol^{-1}

Ionization potential:

$$I = -E_{HOMO} \quad (9)$$

Electron affinity:

$$A = -E_{LUMO} \quad (10)$$

Hardness:

$$\eta = -\frac{I - A}{2} \quad (11)$$

Chemical potential:

$$\mu = -\frac{I + A}{2} \quad (12)$$

Electrophilicity index:

$$\omega = \frac{\mu^2}{2\eta} \quad (13)$$

Softness:

$$\sigma = \frac{1}{\eta} \quad (14)$$

Table-10 reveals the electronic action of DDQ, CHL, CTC1 and CTC2. It may be deduced from the H0MO and LUMO energies that molecules with higher E_{HOMO} values are better electron donors and those with lower E_{LUMO} values are greater electron acceptors. DDQ and CHL are distinguished from 1-CYHP by a lower E_{LUMO} value. On the other hand, 1-CYHP has higher E_{HOMO} value than DDQ and CHL, hence 1-CYHP acted as electron donating group and DDQ and CHL as electron accepting groups in the reaction.

Furthermore, 1-CYHP is found to have a greater chemical potential (μ) value compared to that of DDQ and CHL. As DDQ consist of high electronphilicity index (ω) value when compared to CHL, the former is a better electrophile than the latter. Based on the values of hardness (η), softness (σ) and other parameters, it has been determined that 1-CYHP acts as an electron donor, whereas DDQ and CHL serve as electron acceptors.

Conclusion

Spectrophotometric studies at room temperature in acetonitrile solvent were used to quantify CTC1: [(1-CYHP)(DDQ)] and CTC2: [(1-CYHP)(CHL)] complexes interactions between donor 1-cyclohexylpiperazine and the acceptors (DDQ and CHL) 1:1 stoichiometry were observed for both CT complexes. The formation constant/stability constants (K_{CT}) and molar extinction coefficients (ε_{CT}) of both CT complexes were calculated using the Benesi-Hildebrand approach. Infrared and ^1H NMR was utilized to characterize and validate the development of charge transfer (CT) complexes. Both CT complexes CTC1 and CTC2 have intrinsic binding constants K_b of 3610 M^{-1} and 2791 M^{-1}, respectively. In comparison to CTC2, the CTC1 displays high binding affinity depending on their intrinsic binding affinity data. The charge transfer complexes were also investigated using the DFT methodology for molecular optimization. Finally, the length of bond, angles, Mulliken atomic charge densities, electrostatic potential surface maps, reactive descriptors and HOMO~LUMO energy values of CT complexes were investigated and the experimental findings correlating well with the theoretical findings.

ACKNOWLEDGEMENTS

The authors acknowledge to CVR College of Engineering, Hyderabad, India for providing the research facilities to carry out this work.

CONFLICT OF INTEREST

The authors declare that there is no conflict of interests regarding the publication of this article.

REFERENCES

1. R.S. Mulliken, *J. Am. Chem. Soc.*, **72**, 600 (1950); https://doi.org/10.1021/ja01157a151
2. R.S. Mulliken and W.B. Person, *J. Am. Chem. Soc.*, **91**, 3409 (1969); https://doi.org/10.1021/ja01041a001
3. H. AlRabiah, H.A. Abdel-Aziz and G.A. Mostafa, *J. Mol. Liq.*, **286**, 110754 (2019); https://doi.org/10.1016/j.molliq.2019.04.031
4. F.A. Al-Saif, A.A. El-Habeeb, M.S. Refat, A.M.A. Adam, H.A. Saad, A.I. El-Shenawy and H. Fetooh, *J. Mol. Liq.*, **287**, 110981 (2019); https://doi.org/10.1016/j.molliq.2019.110981
5. M.S. Liao, Y. Lu, V.D. Parker and S. Scheiner, *J. Phys. Chem. A*, **107**, 8939 (2003); https://doi.org/10.1021/jp034985t
6. E.K. Kim and J.K. Kochi, *J. Am. Chem. Soc.*, **113**, 4962 (1991); https://doi.org/10.1021/ja00013a036
7. N. Singh, I.M. Khan, A. Ahmad and S. Javed, *J. Mol. Liq.*, **191**, 142 (2014); https://doi.org/10.1016/j.molliq.2013.12.002
8. A.M.A. Adam and M.S. Refat, *J. Mol. Liq.*, **219**, 377 (2016); https://doi.org/10.1016/j.molliq.2016.03.045
9. A. Eychmüller and A.L. Rogach, *Pure Appl. Chem.*, **72**, 179 (2000); https://doi.org/10.1351/pac200072010179

10. J. Zhang, W. Xu, P. Sheng, G. Zhao and D. Zhu, *Acc. Chem. Res.*, **50**, 1654 (2017); https://doi.org/10.1021/acs.accounts.7b00124
11. P.E. Hansen, P.T. Nguyen, J. Krake, J. Spanget-Larsen and T. Lund, *Spectrochim. Acta A Mol. Biomol. Spectrosc.*, **98**, 247 (2012); https://doi.org/10.1016/j.saa.2012.08.006
12. F. Yakuphanoglu and M. Arslan, *Opt. Mater.*, **27**, 29 (2004); https://doi.org/10.1016/j.optmat.2004.01.017
13. A. Dozal, H. Keyzer, H.K. Kim and W.W. Wang, *Int. J. Antimicrob. Agents*, **14**, 261 (2000); https://doi.org/10.1016/S0924-8579(99)00163-6
14. E.B. Veale and T. Gunnlaugsson, *J. Org. Chem.*, **75**, 5513 (2010); https://doi.org/10.1021/jo1005697
15. M.A. Diab, A.Z. ElSonbati, S.M. Morgan and M.A. ElMogazy, *Appl. Organomet. Chem.*, **32**, e4378 (2018); https://doi.org/10.1002/aoc.4378
16. I.M. Khan, A. Ahmad and M.F. Ullah, *Spectrochim. Acta A Mol. Biomol. Spectrosc.*, **102**, 82 (2013); https://doi.org/10.1016/j.saa.2012.10.027
17. I.M. Khan, A. Ahmad and M. Oves, *Spectrochim. Acta A Mol. Biomol. Spectrosc.*, **77**, 1059 (2010); https://doi.org/10.1016/j.saa.2010.08.073
18. A.S. Gaballa and A.S. Amin, *Spectrochim. Acta A Mol. Biomol. Spectrosc.*, **145**, 302 (2015); https://doi.org/10.1016/j.saa.2015.03.005
19. T.M. El-Gogary, M.A. Diab and S.F. El-Tantawy, *Spectrochim. Acta A Mol. Biomol. Spectrosc.*, **66**, 94 (2007); https://doi.org/10.1016/j.saa.2006.02.029
20. M. Pandeeswaran and K.P. Elango, *Spectrochim. Acta A Mol. Biomol. Spectrosc.*, **65**, 1148 (2006); https://doi.org/10.1016/j.saa.2005.12.037
21. K. Ganesh, C. Balraj, A. Satheshkumar and K.P. Elango, *Spectrochim. Acta A Mol. Biomol. Spectrosc.*, **92**, 46 (2012); https://doi.org/10.1016/j.saa.2012.02.026
22. S.M. Morgan, M.A. Diab and A.Z. ElSonbati, *Appl. Organomet. Chem.*, **32**, e4281 (2018); https://doi.org/10.1002/aoc.4281
23. N. Venkatesh, B. Naveen, A. Venugopal, G. Suresh, V. Mahipal, P. Manojkumar and T. Parthasarathy, *J. Mol. Struct.*, **1196**, 462 (2019); https://doi.org/10.1016/j.molstruc.2019.06.083
24. S.K. Kodadi and P. Tigulla, *J. Solution Chem.*, **46**, 1364 (2017); https://doi.org/10.1007/s10953-017-0643-6
25. A. Lakkadi, N. Baindla and P. Tigulla, *J. Solution Chem.*, **46**, 2171 (2017); https://doi.org/10.1007/s10953-017-0685-9
26. V. Abbu, V. Nampally, N. Baindla and P. Tigulla, *J. Solution Chem.*, **48**, 61 (2019); https://doi.org/10.1007/s10953-019-00847-5
27. H.A. Benesi and J.H.J. Hildebrand, *J. Am. Chem. Soc.*, **71**, 2703 (1949); https://doi.org/10.1021/ja01176a030
28. M.K. Palnati, N. Baindla and P. Tigulla, *J. Solution Chem.*, **47**, 975 (2018); https://doi.org/10.1007/s10953-018-0767-3
29. G. Briegleb and J. Czekalla, *Angew. Chem.*, **72**, 401 (1960); https://doi.org/10.1002/ange.19600721203
30. A.N. Martin, J. Swarbrick and A. Cammarata, Physical Pharmacy, Lee and Febiger, Philadelphia, edn 3, pp 371-374, 344-346 (1983).
31. G.G. Aloisi and S. Pignataro, *J. Chem. Soc*., *Faraday Trans. I*, **69**, 534 (1973); https://doi.org/10.1039/f19736900534
32. M.S. Refat, A. Elfalaky and E. Elesh, *J. Mol. Struct.*, **990**, 217 (2011); https://doi.org/10.1016/j.molstruc.2011.01.049
33. G. Briegleb and J. Czekalla, *Z. Physik. Chem.*, **24**, 37 (1960); https://doi.org/10.1524/zpch.1960.24.1_2.037
34. V. Murugesan, M. Saravanabhavan and M. Sekar, *Spectrochim. Acta A Mol. Biomol. Spectrosc.*, **147**, 99 (2015); https://doi.org/10.1016/j.saa.2015.03.083
35. N. Vamsikrishna, M.P. Kumar, G. Ramesh, N. Ganji, S. Daravath and Shivaraj, *J. Chem. Sci.*, **129**, 609 (2017); https://doi.org/10.1007/s12039-017-1273-7
36. A.M.A. Adam, M.S. Hegab, M.S. Refat and H.H. Eldaroti, *J. Mol. Struct.*, **1231**, 129687 (2021); https://doi.org/10.1016/j.molstruc.2020.129687
37. M. Shukla, N. Srivastava and S. Saha, *J. Mol. Struct.*, **1021**, 153 (2012); https://doi.org/10.1016/j.molstruc.2012.04.075
38. B. Naveen, L. Arunapriya and T. Parthasarathy, *Indian J. Chem. A*, **55**, 1209 (2016).
39. O.R. Shehab and A.M. Mansour, *J. Mol. Struct.*, **1047**, 121 (2013); https://doi.org/10.1016/j.molstruc.2013.04.065
40. A.Z. El-Sonbati, M.A. Diab, S.M. Morgan, M.I. Abou-Dobara and A.A. El-Ghettany, *J. Mol. Struct.*, **1200**, 127065 (2020); https://doi.org/10.1016/j.molstruc.2019.127065
41. Y. Kato, H. Matsumoto and T. Mori, *J. Phys. Chem. A*, **125**, 146 (2021); https://doi.org/10.1021/acs.jpca.0c08925
42. H.M. Refaat, H.A. El-Badway and S.M. Morgan, *J. Mol. Liq.*, **220**, 802 (2016); https://doi.org/10.1016/j.molliq.2016.04.124
43. V. Mahipal, N. Venkatesh, B. Naveen, G. Suresh, V. Manaiah and T. Parthasarathy, *Chem. Data Collect.*, **28**, 100474 (2020); https://doi.org/10.1016/j.cdc.2020.100474
44. G. Suresh, N. Venkatesh, B. Naveen, V. Mahipal, M. Madhavi and T. Parthasarathy, *J. Solution Chem.*, **49**, 777 (2020); https://doi.org/10.1007/s10953-020-00989-x